Arabian Journal of Chemistry (2019) **12**, 1061–1069

King Saud University

Arabian Journal of Chemistry

www.ksu.edu.sa
www.sciencedirect.com

ORIGINAL ARTICLE

Biochemical activities and electronic spectra of different cobalt phenanthroline complexes

Mohammed A. Al-Omair

Department of Chemistry, College of Science, King Faisal University, Al-Hassa 31982, Saudi Arabia

Received 5 June 2018; accepted 6 November 2018
Available online 15 November 2018

KEYWORDS

1,10-Phenanthroline;
Co(II) complexes;
FTIR;
Antibacteria;
Antioxidant;
Anticancer;
Electronic spectra

Abstract A series of octahedral phenanthroline cobalt chlorides, aqua and carbonates complexes have been prepared, characterized, and their antibacterial activity was studied in detail in terms of zone inhibition and minimum inhibitory concentrations. Their antioxidant activities were studied by measuring DPPH, SOD and ABTS radical scavenging activity. It was found that cobalt phenanthroline carbonate complex possessed highest antibacterial activity, antioxidant activity, degradation effect on DNA and showed moderate cytotoxicity against Hepatocellular carcinoma (HEPG-2), Mammary gland (MCF-7) and Colorectal carcinoma (HCT-116) cells.

The complexes were studied with UV spectroscopy to observe the solvents effect on the electronic spectra. Equation that relates peak position λ max to solvent parameters are solved by computerized analysis using multiple regression techniques, and the correlation and regression coefficients were evaluated. The independent solvent parameters used are H-bonding ability, refractive index and dielectric constant. The FTIR spectrum was interpreted according to the actual structure.

1. Introduction

Metal phenanthroline complexes have attracted great attention in modern medicine due to their antibacterial properties (Viganor et al., 2017). The improper uses of antimicrobial drugs lead to high levels of resistance in bacteria. This caused an increase in the number of untreatable bacterial infections coupled with the emergence of strains resistant to almost all drugs (Tomasz, 1994; Juan et al., 2018). World health organization "WHO" dispatch very high occurrence of bacteria resistance like in *Escherichia coli, Klebsiella pneumoniae, Staphylococcus aureus, Streptococcus pneumoniae, Shigella, Neisseria gonorrhoeae, and Mycobacterium tuberculosis* to several well existing antibiotics drugs such as cephalosporin, penicillin and fluoroquinolones, and rifampicin. This situation constitutes a major problem and addresses a risk to public health and economic anxiety to countries worldwide (Tanwar et al., 2014; Nikaido, 2009). Clearly there is a need for fighting against these resistant pathogens and development of new classes of antibiotics capable of killing bacteria through pathways that are different from classical antibacterial drugs.

Transition metal complexes with biologically active ligands are the basis for the production of new active drugs. 1,10-phenanthroline metal complexes are of great interest as anticancer agent because they act as models for biological systems

E-mail address: alomair@kfu.edu.sa
Peer review under responsibility of King Saud University.

Production and hosting by Elsevier

https://doi.org/10.1016/j.arabjc.2018.11.006
1878-5352

like binding of small molecules to DNA (Mohammad et al., 2015). These heterocyclic aromatic ligands containing coordinating nitrogen atom, can adopt π–π stacking interactions which mimic various biological processes (Michael et al., 2007). 1,10-phenanthroline shows *in vitro* antimicrobial activity against a wide range of bacteria. The development of metal 1,10-phenanthroline complexes offers biochemist an opportunity to widen structural possibilities and controlling geometries by inclusion of proper auxiliary ligands and counter ions. This could provide the chance to hit various biochemical paths in bacteria. Preparation and antibacterial activities of new cobalt(II) complexes with 1,10-phenanthroline and 2,2′-bipyridine mixed ligands was reported (Agwara et al., 2010). New Co(II) complex with 1,10-Phenanthroline imidazole derivative have been prepared, characterized and was screened for antibacterial activity against several bacterial strains (Mesut et al., 2013). Cobalt(III) mixed ligand complexes of the type $[Co(en)_2L]^{+3}$, where en is ethylene diamine and L is bipyridine or 1,10-phenanthroline were prepared and proved to be potential antimicrobial agents (Penumaka et al., 2006).

Recently $[Co(phen)_3](NO_3)_2]\cdot 2H_2O$ and $[Co(phen)_2(N_3)_2]NO_3$ were synthesized, tested for *in vitro* antimicrobial activities and proved to be good antibacterial candidates (Djuikom et al., 2016). The solubility and stability of complex in appropriate solvent are essential factors in the delivery of biologically active molecules to its targets and fulfilling its goal as antibacterial agents. Although UV–vis spectra of metal complexes have been explored in recent years, only rare information is available about the effect of various solvent parameters on the location of their maximum absorption wavelength λ max (Mamdouh et al., 2011; Dong et al., 2018).

In the contest of investigating the good biological effects of cobalt phenanthroline complexes, we report here the synthesis and FTIR spectral elaboration of cobalt(II) complexes of 1,10-phen with chloro, aqua and carbonates co-ligands. The influence of co-ligands on the biological activities of cobalt phenanthroline complexes towards some resistant pathogens are evaluated using *in vitro* assays. Antioxidant activity, cleavage of DNA and cytotoxicity of complexes are also investigated. Correlation data was computed to estimate solvent–solute interaction effects on the UV electronic absorption spectra of cobalt phenanthroline complexes.

2. Experimental

2.1. Chemicals and instruments

Chemicals were Merck and Sigma products. Sodium carbonates, 1,10-phenanthroline (**AO-A**), cobalt dichloride hexahydrates (**AO-B**), cobalt sulfate heptahydrate (**AO-C**). All organic solvents used were of spectroscopic quality (>99.8%). The cell lines HEPG-2, MCF-7 and HCT-116 were purchased from ATCC from "Holding" company for biological products and vaccines (VACSERA), Cairo, Egypt.

FT-IR reflectance spectra were recorded by using Shimadzu Infrared Spectrophotometer (FT-IR-8300) in the range (4000–400) cm^{-1}. UV–Vis spectra of cobalt phenantholine complexes were determined on Shimadzu UV–Vis spectrophotometer.

2.2. Synthesis of complexes

The octahedral complexes (Fig. 1) were prepared according to the methods described in the literature with some modification:

$CoCl_2\cdot 6H_2O$ (5.9 mmol) and phenanthroline (3 mmol) were mixed in 40 ml acetonitrile, a blue powder completely precipitated after 3 h, filtered, collected, washed with little acetonitrile and dried giving $[Co(phen)_2Cl_2].1.5\ CH_3CN$ (**AO-2**) (1.64 mmol) (28% yield).

$[Co(phen)(H_2O)_4]SO_4\cdot 2H_2O$ (**AO-3**) was prepared by mixing $CoSO_4\cdot 7H_2O$ (3.56 mmol), phenanthroline (3.56 mmol) in 20 ml water for 2 h, the obtained pink powder was collected by filtration, washed with water and dried to give **AO-3** (2.03 mmol) (57% yield).

$CoCl_2\cdot 6H_2O$ (2 mmol), phenanthroline (4 mmol) and sodium carbonate (4 mmol) were mixed in 20 ml water for 2 h, the precipitated orange powder was collected, washed with little water and ethanol and dried giving $[Co(phen)_2CO_3].7H_2O$ (**AO-5**) (1.16 mmol) (58% yield).

The structures shown in Fig. 1 are redrawn based on reported structures obtained by single X-ray diffraction analysis (CIF files) of the crystals of complexes: $[Co(phen)_2Cl_2].1.5\ CH_3CN$ (**AO-2**) (Alan et al., 1997); $[Co(phen)(H_2O)_4]SO_4\cdot 2H_2O$ (**AO-3**) (Zhu et al., 2002); $[Co(phen)_2CO_3].7H_2O$ (**AO-5**) (Li et al., 2004).

2.3. Electronic spectral studies

The electronic spectra were recorded on a Shimadzu Spectrophotometer using 1 cm quartz cell at 25 °C. The electronic spectra of the solutions of complexes (concentration 1×10^{-5} to 1×10^{-6} mol/L) were investigated in water and organic solvents of various polarities: methanol, ethanol, acetonitrile, *N*, *N*-dimethylformamide (DMF), and dimethylsulfoxide (DMSO).

2.4. Antibacterial test

The antimicrobial evaluation of the tested ligands (**AO-A**, **AO-B**, **AO-C**) and their complexes (**AO-2**, **AO-3**, **AO-5**) were carried out *via* cup diffusion technique (Youssef et al., 2016).

Minimal inhibitory concentration (MIC) values of **AO-A, AO-B, AO-C, AO-2, AO-3** and **AO-5** compounds were studied according to micro well dilution method (Kavanagh, 1963).

2.5. Antioxidant activity

Estimation of antioxidant activities of Co complexes using DPPH: Radical scavenging activity of compounds **AO-A, AO-B, AO-C, AO-2, AO-3** and **AO-5** against stable 2, 2-diphenyl-1-picrylhidrazine (DPPH) was estimated by UV/visible light spectrophotometery according to (Mensor et al., 2001).

Determination of Superoxide Dismutase (SOD) like activity: **AO-A, AO-B, AO-C, AO-2, AO-3** and **AO-5** were assayed for superoxide dismutase enzyme SOD like activity using phenazenemethosulphate (PMS) to generate a superoxide anion radicals at pH = 8.3 (phosphate buffer) as reported (Bridges and Salin, 1981).

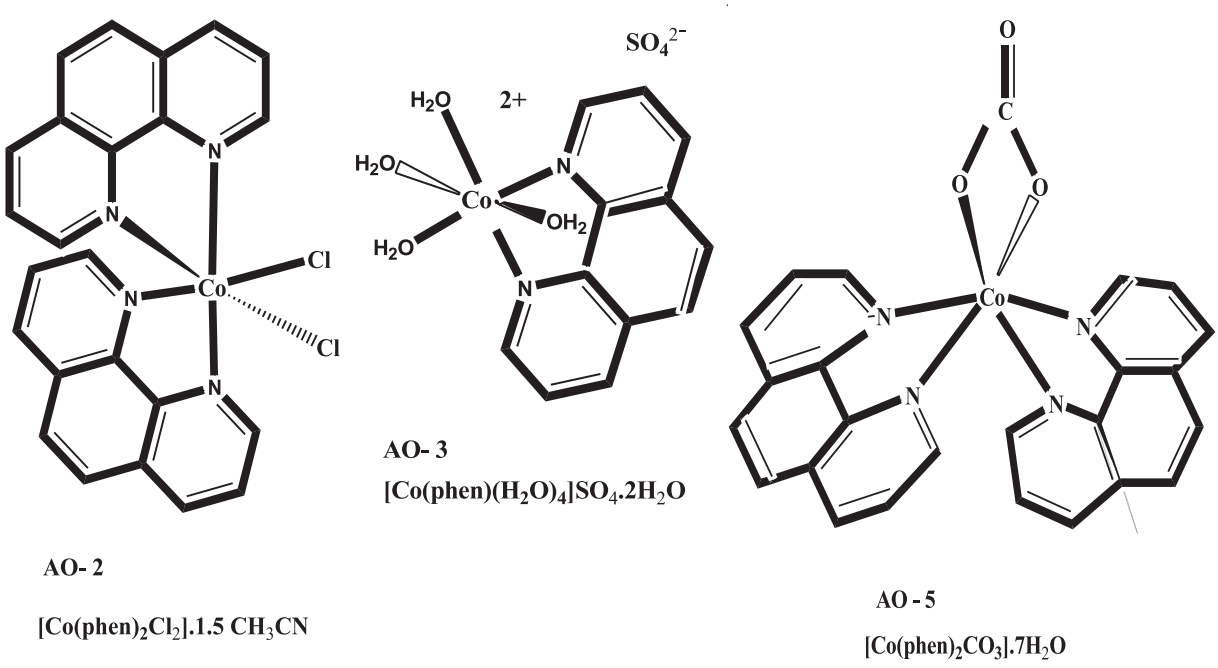

Fig. 1 Structures of cobalt phenanthroline complexes.

ABTS radical cation decolorization assay: ABTS [(2,2′-azino-bis-3-ethylbenzthiazoline-6-sulphonic acid) diammonium salt] forms a relatively steady free radical which is decolorized in its non-radical form. The evaluation of ABTS free radical scavenging activity was assessed spectrophotometrically as reported (Re et al., 1999).

2.6. Agarose gels electrophoresis

The **AO-A, AO-B, AO-C, AO-2, AO-3** and **AO-5** (20 μg) were added individually to 1 μg of the DNA isolated from *E. coli* strain W3110 (Youssef and Al-Omair, 2008). The DNA was visualized on a UV transilluminator after staining the agarose gels with ethidium bromide (0.5 μg/ml) (Sambrook et al., 1989).

2.7. Cytotoxicity assay

Doxorubicin was used as a reference anticancer drug for comparison. The cell lines stated above were utilized to evaluate the inhibitory effects of the ligands and metal salts (**AO-A**, **AO-B**, **AO-C**), and the complexes (**AO-2**, **AO-3**, **AO-5**) according to the reported method (Elghamry et al., 2017).

3. Results and discussion

3.1. FTIR studies

The strong bands at 732.2 cm^{-1} and 839.9 cm^{-1} have been assigned to out of plane C—H deformation motion on the heterocyclic rings, and on the center ring respectively of phenanthroline **AO-A**. There is a decrease of ≈10 cm^{-1} in the wavenumbers of the first band due to co-ordination of nitrogen atom. It appears at 722.2, 723.6 and 721.9 cm^{-1} for complex **AO-2**, **AO-3** and **AO-5** respectively, Fig. 2. The band at 839.9 cm^{-1} band is affected upon coordination in the opposite way. An increase in wavenumbers is observed at 852.2, 845.5 and 844.8 cm^{-1} for complexes **AO-2**, **AO-3** and **AO-5** respectively. The bands in the region 1135.8 and 1215.8 cm^{-1} are referred to in-plane hydrogen deformation motions or possibly ring vibrations. There has been a shift to 1142.6 and 1197.9 cm^{-1} in **AO-2** and to 1145.9 cm^{-1} in **AO-5**.

Most intense and characteristic bands in the vibrational spectrum of phenanthroline occur in the range 1400–1600 cm^{-1}. All of these bands involve ≻C═C≺ and ≻C═N stretching vibrations, and upon co-ordination move to higher frequencies. The strong peak at 1416.8 cm^{-1} due to in plane

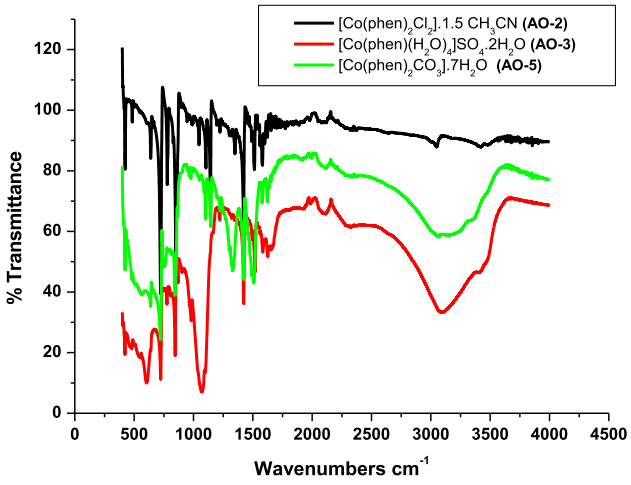

Fig. 2 FTIR spectra of $[Co(phen)_2Cl_2].1.5\ CH_3CN$ (**AO-2**), $[Co(phen)(H_2O)_4]SO_4{\cdot}2H_2O$ (**AO-3**) and $[Co(phen)_2CO_3].7H_2O$ (**AO-5**).

antisymmetric ring deformation involving >C=C< and >C=N stretching modes, slightly increases upon coordination to 1421.4 **AO-2**, 1423.1 (**AO-3**) and 1424.5 cm^{-1} (**AO-5**). While a prominent increase in wavenumber by 13–20 cm^{-1} occurs at 1498.0 cm^{-1} for the symmetric ring stretching mode peak to 1513.2 (**AO-2**), 1518.5 (**AO-3**) and 1510.9 cm^{-1} (**AO-5**). This is expected as coordination takes place at nitrogen atom of the >C=N (phenanthroline ring) groups to cobalt(II) ion, and the effect is transmitted throughout the region resulting into the readjustment of electron density (Mashaly et al., 2005).

The strong and very broad bands spread from 2600 to 3500 cm^{-1} and centered at 3116.56 and 3069.87 cm^{-1}, are due to OH stretching vibrations of coordinating and crystalline H_2O molecules in **AO-3** and of crystalline H_2O in **AO-5** (El-Sherif et al., 2012; Masoud et al., 2012). In the lower wavenumber region, the weak bands observed for the three complexes at 423 cm^{-1} have been assigned to ν(M—N) vibrations while the weak bands observed at 600.0 and 571.0 cm^{-1} have been assigned to ν(M—O) of **AO-3** and **AO-5** respectively (Ali et al., 2010).

Conclusive evidence regarding bonding of two oxygen atoms of carbonate ligand to cobalt ions in **AO-5** is the considerable change in IR peak position of carbonate to lower wave number upon complexation with metal ion. The O—C=O stretching vibrations at 1755 cm^{-1} and 1440 cm^{-1} of sodium carbonates are shifted to lower frequencies 1510.92 and 1333.5 cm^{-1} in the complexes. Finally, the very strong peak at 1142.6 cm^{-1} confirm the presence of sulfate counter ion in complex **AO-3**, Fig. 2 (Miller and Wilkins, 1952).

3.2. Antibacterial activities

The antimicrobial activities of the compounds **AO-A, AO-B, AO-C, AO-2, AO-3** and **AO-5** are tested against both Gram-negative and Gram-positive bacteria with similar concentration in DMSO. The inhibition zone against the growth of the microorganisms by the compounds **AO-A, AO-B, AO-C, AO-2, AO-3** and **AO-5** are given in Table 1, Fig. 3. It is confirmed that among the tested compounds **AO-A, AO-C** and **AO-5** exhibit the most antimicrobial activities toward all microorganisms, and are little less than the reference antibiotic ampicillin. The tested compounds **AO-B** and **AO-3** revealed good antimicrobial activity toward the examined microorganisms while compound **AO-2** reveal the lowest antimicrobial activity all over the study.

Table 1 Effects of **AO-A, AO-B, AO-C, AO-2, AO-3** and **AO-5** compounds on Gram-negative and Gram-positive microorganisms. The results are expressed as diameter of zone inhibition in (mm).

	Gram-negative		Gram-positive	
	E. coli	*P. aeruginosa*	*S. aureus*	*B. megaterium*
AO-A	17	16	20	19
AO-B	16	14	17	16
AO-C	17	18	20	20
AO-2	13	12	14	12
AO-3	15	14	16	13
AO-5	17	18	19	20
Ampicillin	19	20	23	21

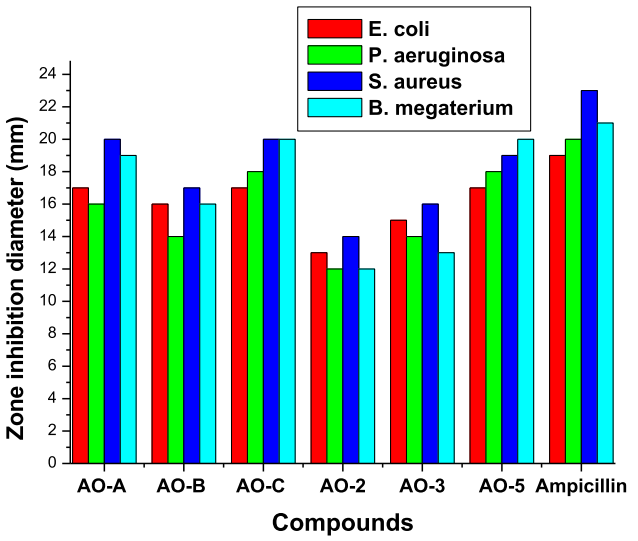

Fig. 3 The inhibition zone diameter (mm) of various compounds and reference ampicillin at the same concentration for different gram-negative and gram positive-bacteria.

Comparison of minimum inhibitory concentration MICs (in μg/mL) of compounds and the standard drug ampicillin against susceptible Gram-negative and Gram-positive bacterial strains are represented in Table 2. It was found that compound **AO-A, AO-C** and **AO-5** exhibited the highest inhibitory activity against all bacteria with MIC ranging from 15 to 35 μg/mL. Compounds **AO-B** and **AO-3** had good inhibitory activity against all strains (MIC: 30–55 μg/mL). On the other hand, compound **AO-2** has low inhibitory activity toward the tested bacterial strains (MIC: 55–70 μg/mL). This suggests that the antibacterial activity of compounds is dependent on the basic structure as well as the nature of the ligands and counterions of the formed complex. In general, it can be also inferred that the complexes have more inhibitory activity towards gram negative bacteria than gram positive bacteria.

MIC was also calculated in μmol/ml (Table 2 and Fig. 4) to compare antibacterial activity with respect to stoichiometric relation of moles for different complexes and their metal ion and ligands.

It was found that MIC in (μmol/l) of the complexes are lower than the corresponding starting metal salts AO-B and AO-C. Indicating enhancement of antibacterial activity of complexes due to incorporation of phenanthroline ligand in their structures. **AO-5** being the most potent antibacterial agent with MIC (μmol/l) value close to that of ampicillin. It was found that MIC in μmol/L for complex **AO-5** for example is smaller than its corresponding phenanthroline ligand **AO-A** and metal ion salt cobalt chloride **AO-B**.

3.3. Antioxidant activity

The production of free radicals, reactive oxygen species (ROS) and reactive nitrogen species (RNS) is inevitable during oxidative metabolic process. High concentrations of these reactive molecules in the cells induce denaturation and deterioration

Table 2 Minimum inhibitory concentration μmol/ml and (μg/ml) of **AO-A, AO-B, AO-C, AO-2, AO-3** and **AO-5** compounds against Gram-negative and Gram-positive microorganisms.

	Gram-negative		Gram-positive	
Compound number	*E. coli*	*P. aeruginosa*	*S. aureus*	*B. megaterium*
AO-A	0.0832 (15)	0.111 (20)	0.111 (20)	0.111 (20)
AO-B	0.168 (40)	0.126 (30)	0.189 (45)	0.231 (55)
AO-C	0.107 (30)	0.124 (35)	0.124 (35)	0.124 (35)
AO-2	0.109 (60)	0.127 (70)	0.0997 (55)	0.109 (60)
AO-3	0.101 (45)	0.101 (45)	0.124 (55)	0.113 (50)
AO-5	0.0413 (25)	0.0578 (35)	0.0498 (30)	0.0578 (35)
Ampicillin	0.0286 (10)	0.0429 (15)	0.0429 (15)	0.0429 (15)

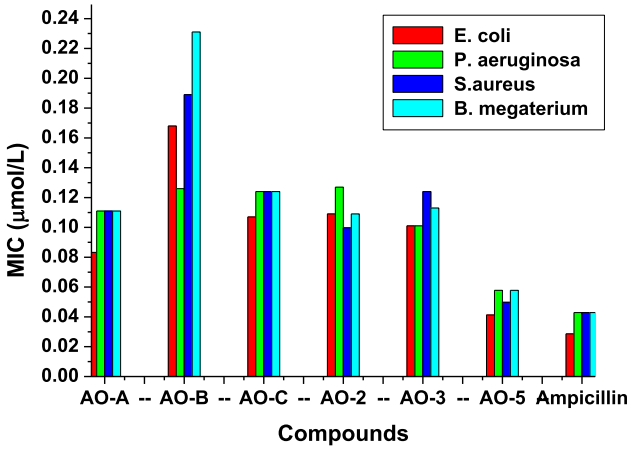

Fig. 4 Histogram of MIC (μmol/ml) of compounds against bacteria species.

Table 3 Radical scavenging activity of the tested compounds **AO-A, AO-B, AO-C, AO-2, AO-3** and **AO-5** as antioxidant agents.

Compounds	DPPH radical scavenging activity	SOD mimetic superoxide scavenging catalytic activity	ABTS radical scavenging
AO-A	63.4 ± 0.57	68.2 ± 0.71	63.8 ± 0.57
AO-B	47.8 ± 0.76	52.6 ± 0.84	46.7 ± 0.52
AO-C	61.8 ± 0.81	65.1 ± 0.66	64.8 ± 0.71
AO-2	37.5 ± 0.78	41.8 ± 0.62	46.9 ± 0.43
AO-3	45.9 ± 0.81	50.7 ± 0.73	48.2 ± 0.67
AO-5	59.7 ± 0.73	63.7 ± 0.84	62.5 ± 0.75

of many cellular components. This results in cellular oxidative stress and consequently cancer.

DPPH free radical scavenging activity: In a typical antioxidant activity study, the radical scavenging activity (RSA) of compounds can be rapidly screened by evaluation of DPPH· RSA. The compounds showed antiradical activity by inhibiting DPPH radical (Table 3). Most of analyzed compounds revealed high to moderate interaction with DPPH radical at a concentration of 2 μg/mL. The maximum antioxidant activity was found in compounds in the following order **AO-A** > **AO-C** > **AO-5** with inhibitions greater than 50% and is comparable to standard vitamin C (78.6 ± 0.88) while other compounds showed moderate RSA in the order **AO-B** > **AO-3** > **AO-2**, Table 3. The antioxidant activity of these compounds is caused by their electron donating ability to DPPH radical.

SOD mimetic scavenging catalytic activity: Based on DNA binding capability of the compounds **AO-A, AO-B, AO-C, AO-2, AO-3** and **AO-5** compounds, it is beneficial to study the antioxidant activity of these compounds. Superoxide radical anions ($O_2^{\cdot-}$) generates dynamic free radicals that react with biomolecules and cause cell deterioration. In this colorimetric method, the reduced NBT to blue formazan was utilized as a marker of $O2^{\cdot-}$ generation and detected at 560 nm (Youssef et al., 2016). SOD - mimetic superoxide scavenging catalytic activity by the tested compounds was detected by their inhibition of reduction of NBT to formazan by decreasing the superoxide ion concentration. The tested compounds compete with NBT for oxidation of the generated superoxide ions. The tested compounds **AO-A, AO-C** and **AO-5** exhibited the greatest antioxidant activities with % inhibition of 68.2 ± 0.71, 65.1 ± 0.66 and 63.7 ± 0.84 respectively. While compounds AO-B and AO-3 displayed good SOD like activity within % inhibition greater than 50% as shown in Table 3. Horse radish (82.4 ± 0.57) was evaluated as standard for comparison.

ABTS radical cation decolorization assay: The antioxidant activity is based on color intensity reduction of free radical cation at 734 nm from ABTS solution due to radical scavenging by antioxidant material. The importance of ABTS derived free radical method is that the reaction is stoichiometric and the color is stable for more than 1 h (Chyong et al., 2011). The results obtained in Table 3 with the control (77.3% ± 0.89) indicated that the antioxidant power of the tested compounds was high in accordance with DPPH and SOD results. The tested compounds **AO-A, AO-C** and **AO-5** showed >50% inhibition of ABTS radical cation, while **AO-B, AO-2** and **AO-3** had weak scavenging activities with inhibition of ABTS less than 50%, Table 3.

Trends in antioxidant activity: **AO5** showed greater antioxidant activity than other complexes. This can be explained by the ease of Co(II) in **AO5** to undergo oxidation to Co(III) and providing an electron to the free radical and thus causing its reduction as observed in DPPH, SOD and ABTS radical scavenging catalytic activity. The produced $[Co(III)(phen)_2CO_3]^+$ complex is stable (Omer et al., 2010) and the antioxidant

activity of AO5 can thus be explained by its behavior as a reducing agent according to the following reaction:

$$[Co(II)(phen)_2CO_3]\ (\mathbf{AO5}) \rightleftharpoons\rightleftharpoons [Co(III)(phen)_2CO_3]^+ + e-$$

3.4. DNA affinity and DNA cleavage ability

Agarose gel electrophoresis was used to study the ability of compounds to cleave genomic DNA as one possible mechanism of interaction. The tested compounds **AO-A**, **AO-C**, and **AO-5** displayed DNA degradation effect in a concentration dependent manner due to their binding affinity to DNA. The cleavage of DNA by the compounds **AO-A, AO-B, AO-C, AO-2, AO-3** and **AO-5** was found to increase with increase in concentrations from 2, 4, 6 to 8 μM (Fig. 5). The results indicated that at 2 μM all compounds caused negligible degradation of DNA. Raising the concentration of compounds **AO-A**, **AO-C** and **AO-5** to 4 μM showed noticeable degradation effect on DNA. The tested compounds **AO-B** and **AO-3** caused an efficient cleavage ability of DNA at 6 μM concentration. Furthermore, all compounds **AO-A**, **AO-B**, **AO-C**, **AO-2**, **AO-3** and **AO-5** demonstrated a good cleavage power of DNA at a concentration of 8 μM (Fig. 5).

Although we expected that Cobalt (II) phenanthroline aqua complex (**AO3**) (Fig. 1) to have the highest binding effect to DNA moieties, because its labile water ligands can be lost and provide an empty d- orbital in the Lewis acid cobalt (II) ion. The ion can bind to electron rich nucleic base moieties in DNA and causes its cleavage. However, since Cobalt (II) phenanthroline carbonates (**AO5**) (Fig. 1) showed the highest cleavage power of DNA, the cleavage mechanism can be due to proper geometry of two phenanthroline ligands in complex (**AO5**) which causes them to interact strongly with heterocylic aromatic ring of DNA through π–π interactions.

3.5. Cytotoxicity evaluation

Hepatocellular carcinoma (HEPG-2), Mammary gland (MCF-7) and Colorectal carcinoma (HCT-116) cells (Table 4) were used in cytotoxicity test to evaluate anti-proliferative activities of the ligands and metal salts (**AO-A**, **AO-C**, **AO-B**), and the complexes (**AO-2**, **AO-3**, **AO-5**). Doxorubicin was utilized as a standard anticancer agent since it gives a very strong anticancer activity. As illustrated in Table 4, phenanthroline ligand (AO-A**)** has high anticancer activities against cell lines HePG-2, HCT-116 and MCF-7 with IC50 values of 17.82 ± 0.5, 14.65 ± 0.7 and 19.94 ± 0.6 (μM), respectively. The cobalt sulfates salt **AO-C** and cobalt phenanthroline carbonate complex **AO-5** exhibited moderate anticancer activities against all studied cell lines HePG-2, HCT-116 and MCF-7. The salt cobalt dichloride **AO-B**, cobalt (II) phenanthroline chloride acetonitrile (**AO-2**) and cobalt(II) phennthroline aqua sulfate (**AO-3**) displayed weak anticancer activities against all cell lines, Table 4. Although, it is expected that the complexes (**AO2**) and (**AO3**) to show noticeable cytotoxicity because they contain labile ligands chloride and water respectively. The loss of mobile ligand can poromote the formation of empty orbital in cobalt (II) that can bind to DNA nucleic bases. It could be that other factors impede biological activity of these two complexes such as dispersion and stability in physiological medium as well as cell penetration and targeting tumor cells. The activity can be improved by adding an agent that can noncovalently bond to complexes and help in maintaining their suspension and stability in cell media and increase their targeting and penetration ability of tumor cells. Cobalt phenanthroline aqua complex (**AO5**) shows a better cytotoxicity may be because it is more stable and more soluble in the tested medium and can thus reach easily and interact with the target DNA in the anticancer cell.

3.6. Solvent effect on electronic absorption spectra

The maximum absorption peak location **Y** (λ max, nm) of phenanthroline cobalt complexes in a specific solvent (Fig. 6) has been estimated by the following multi-parameter equation (Eq. (1)) (Hassan et al., 2006):

$$\boldsymbol{Y = a0 + a1X1 + a2X2 + a3X3 + a4X4 + \ldots + anXn.} \quad (1)$$

Equation (Eq. (1)) is solved for the intercept ***a0*** and the coefficient ***ai*** using multiple regression techniques. ***Y*** is used as the dependent variable, while the solvent interaction mechanisms are taken as the independent variables ***Xi,*** and designated as ***E, K, M*** and ***N*** with equation (Eqs. (2)–(5)) listed in (Table 5). ***E*** (Eq. (2)) is the empirical solvent polarity and depends on both solute–solvent hydrogen bonding and dipolar interactions. ***K*** (Eq. (3)) is a measure of the polarity of the

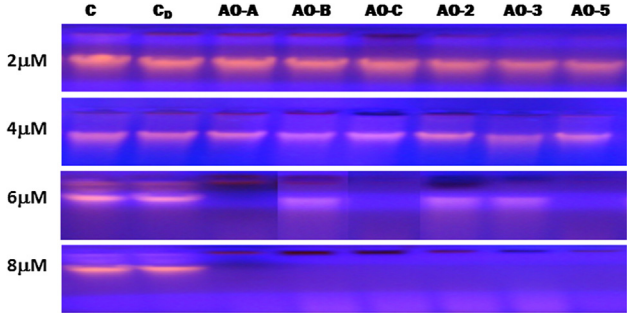

Fig. 5 A figure showing the degradation effect of 2, 4, 6 and 8 μM of compounds **AO-A**, **AO-B**, **AO-C**, **AO-2**, **AO-3** and **AO-5** (Lanes 3–8) on the genomic DNA isolated from *E. coli* Lane1 *E. coli* DNA; lane 2 *E. coli* DNA + DMSO.

Table 4 Cytotoxic activity of synthesized compounds (μM) against human tumor cells.

Compounds	In vitro cytotoxicity IC50 (μM)[a]		
	HePG-2	HCT-116	MCF-7
DOX[b]	5.42 ± 0.3	6.53 ± 0.4	5.28 ± 0.3
AO-A	17.82 ± 0.5	14.65 ± 0.7	19.94 ± 0.6
AO-B	55.47 ± 1.8	61.63 ± 1.6	59.34 ± 1.4
AO-C	24.48 ± 1.3	25.64 ± 2.2	27.47 ± 2.0
AO-2	60.51 ± 1.1	52.96 ± 1.3	56.57 ± 1.5
AO-3	56.67 ± 2.4	68.82 ± 2.6	76.13 ± 2.7
AO-5	35.23 ± 2.3	24.73 ± 1.4	37.92 ± 1.4

[a] IC50 (μM):1–10 (very strong). 11–20 (strong). 21–50 (moderate). 51–100 (weak) and above 100 (non-cytotoxic).
[b] DOX: Doxorubicin.

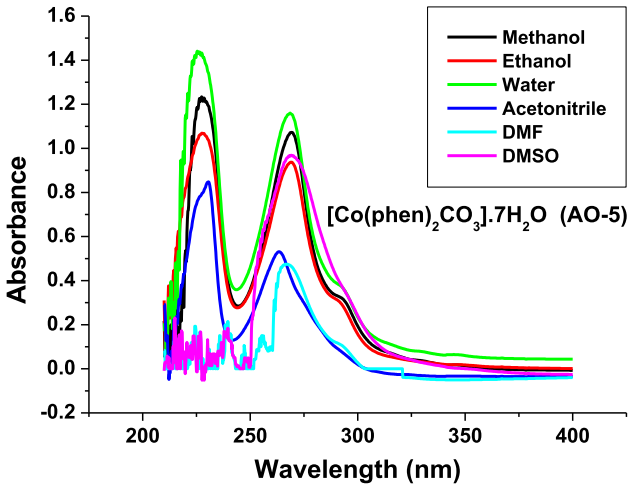

Fig. 6 UV Absorption spectra of $[Co(phen)_2CO_3].7H_2O$ (**AO-5**) in different solvents. Absorbance vs. wavelength (nm).

solvent and depends on the solvent dielectric constant ***D*** (Eq. (4)). While ***M*** (Eq. (5)) depends on the solvent refractive index ***n*** and estimates solute permanent dipole–solvent induced dipole interactions. ***N*** is a measure of permanent dipole–permanent dipole interactions. A multiple regression analysis has been performed using SPSS 23 software. In each case fits are obtained as a function of one parameter, two parameters, or three parameters. The results are presented in Tables 6–8.

All the cobalt (II) complexes studied contain phenanthroline ligand, their UV spectra were recorded in different solvents Fig. 6. The λmax at 269 nm for all three complexes shifts to longer wavelengths with increase in the values of parameters ***E*** and ***D*** i.e. increase in hydrogen bonding ability and polarity of the solvent. This is due to the more stabilization of the exited state than that of the ground state. Thus, the energy difference between excited and unexcited states is slightly reduced, resulting in a small red shift which suggests that the obtained absorption peaks are caused by π–π^* electronic transition of phenanthroline ligand.

Based on the obtained values of correlation coefficients for ***E***, ***K***, ***M*** or ***N*** for the studied one parameter equation, there is strong dependence of the shift in ***λ*max** of **AO-2** on ***M*** and to lesser extent on ***K*** for both complexes **AO-2** and **AO-3** (Table 6 and 7). This indicates that the refractive index of the solvent has greater effect on the absorption peak position than the solvent dielectric constant while ***λ*max** of **AO-5** shows strong dependence on ***E*** (Table 8).

There is improvement in the fit in going from one parameter, two, three to four parameters equation since the multiple correlation coefficients MCC are getting more positive.

Table 5 Solvent dielectric constant ***D***, refractive index ***n***, parameters ***E***, ***K***, ***M***, and ***N***, and observed λ max (nm) values for the complexes in different solvents.

Solvent	*E*	*D*	*n*	*M*	*N*	*K*	λ_{max} AO-2	λ_{max} AO-3	λ_{max} AO-5
Water	63.1	78.5	1.333	0.17	0.76	0.49	269.2	269.2	268.4
Methanol	55.5	32.6	1.329	0.17	0.71	0.48	270	269.6	269.4
Ethanol	51.9	24.3	1.361	0.18	0.67	0.47	270	269.6	269.4
Acetonitrile	46	37.5	1.344	0.18	0.71	0.48	269	268.8	263.4
DMF	43.8	36.7	1.427	0.2	0.67	0.48	269.8	269	266.6
DMSO	45	48.9	1.478	0.22	0.66	0.49	272.2	271.6	269.0
* Solvent parameters		Eq. (2)		Eq. (3)		Eq. (4)		Eq. (5)	
		$E = 2.859 \times 10^{-3} \times v$		$K = \frac{(D-1)}{(2D+1)}$		$M = \frac{(n^2-1)}{(2n^2+1)}$		$N = \frac{D-1}{D+2} - \frac{n^2-1}{n^2+2}$	

Table 6 Regression analysis for **AO-2** using ***E***, ***K***, ***M*** and ***N*** solvent parameters.

Parameters	*a0*	*a1*	*a2*	*a3*	*a4*	*MCC*
E	273.01	−0.059				0.384
K	246.80	48.235				0.318
M	261.28	46.90				0.808
N	283.64	−19.53				0.646
E, K	244.03	−0.070	61.42			0.553
E, M	253.78	0.072	67.33			0.869
E, N	287.48	0.063	−29.63			0.690
K, M	256.38	10.68	45.61			0.811
K, N	241.15	98.93	−26.93			0.885
M, N	264.19	42.58	−3.02			0.811
E, K, M	268.67	0.111	−41.18	83.23		0.890
E, K, N	241.51	0.101	112.49	−44.22		0.963
E, M, N	265.17	0.122	56.83	−17.18		0.922
K, M, N	206.78	293.20	−107.45	−83.13		0.948
E, K, M, N	222.20	0.074	217.48	−60.08	−71.01	0.976

Table 7 Regression analysis for **AO-3** using ***E***, ***K***, ***M*** and ***N*** solvent parameters.

Parameters	*a0*	*a1*	*a2*	*a3*	*a3*	*MCC*
E	271.18	−0.03				0.224
K	243.00	55.29				0.410
M	262.81	36.55				0.708
N	278.75	−13.08				0.487
E, K	241.33	−0.042	63.24			0.512
E, M	253.44	0.09	62.07			0.838
E, N	282.92	0.068	−24.06			0.569
K, M	249.97	27.97	33.18			0.735
K, N	238.79	93.01	−20.04			0.804
M, N	260.44	40.07	2.46			0.711
E, K, M	262.61	0.114	−25.33	71.85		0.848
E, K, N	239.17	0.105	107.06	−37.94		0.916
E, M, N	261.45	0.126	54.69	−12.07		0.873
K, M, N	206.63	274.84	−100.57	−72.64		0.879
E, K, M, N	224.01	0.083	189.50	−47.18	−58.98	0.927

Table 8 Regression analysis for **AO-5** using ***E***, ***K***, ***M*** and ***N*** solvent parameters.

Parameters	*a0*	*a1*	*a2*	*a3*	*a4*	*MCC*
E	260.57	0.14				0.446
K	262.60	10.59				0.034
M	267.12	3.10				0.026
N	272.97	−7.57				0.122
E, K	268.26	0.143	−16.29			0.449
E, M	233.57	0.324	94.51			0.693
E, N	303.68	0.502	−88.29			0.941
K, M	263.03	8.92	2.03			0.038
K, N	260.56	28.91	−9.73			0.149
M, N	280.91	−17.37	−14.31			0.155
E, K, M	325.22	0.563	−253.40	192.37		0.902
E, K, N	262.49	0.536	100.79	−101.37		0.985
E, M, N	285.31	0.551	46.79	−78.04		0.972
K, M, N	123.14	805.75	−429.66	−234.56		0.672
E, K, M, N	223.31	0.481	313.78	−121.88	−155.71	0.997

The ***MCC*** coefficients are good for **AO-2** and **AO-3** complexes while the coefficients for **AO-5** are poor for one parameters equations. When using two parameters (***E, N***) equation the correlation obtained is 0.941, indicating the great influence of solvent empirical polarity and permanent dipoles-dipoles interactions on $\boldsymbol{\lambda}$ **max**. Acceptable correlation for **AO-5** are observed only in going to three and four parameters equations. Tables 6–8 also lists the coefficients for the multi-parameters regression analysis when using three-parameter equations ***E***, ***K***, ***M*** or ***N*** parameters.

The value of ***a0*** is the intercept. The solvent effects due to ***E***, ***K***, ***M*** or ***N*** parameters produce bathochromic shift for positive values of coefficients ***ai***, and hypsochromic shift for negative values of the coefficients.

4. Conclusion

A series of phenanthroline cobalt chlorides, aqua and carbonates complexes have been prepared and characterized. Investigation into the biological activities of this class led to discovery of their antimicrobial, antioxidant and anticancer ability.

It can be concluded that the complexes have more inhibitory activity towards gram negative bacteria than gram positive bacteria. It was found MIC (μmol/l) of the complexes are lower than the corresponding starting metal salts. Enhancement of antibacterial activity of complexes is caused by incorporation of phenanthroline ligand in their structures. Cobalt phenanthroline carbonate complex $[Co(phen)_2CO_3].7\text{-}H_2O$ (**AO-5**) was the most potent antibacterial agent with MIC (μmol/l) value close to that of ampicillin. The antioxidant activity was studied in accordance of DPPH, SOD and ABTS radical scavenging activity. It was found that Phenanthroline cobalt carbonate complex possessed the highest antioxidant activity and degradation effect on the tested DNA. Cobalt phenanthroline aqua complex **AO5** also showed moderate cytotoxicity against Hepatocellular carcinoma (HEPG-2), Mammary gland (MCF-7) and Colorectal carcinoma (HCT-116) cells.

The solvent effect on the wavelength of maximum absorbance peaks $\boldsymbol{\lambda}_{\mathbf{max}}$ of the complexes was studied by regression analysis and high positive correlation coefficients were found. The multi-parameter equations gave higher multiple correlation coefficient values. This indicates that the used empirical

expressions are successful in evaluating solvent effect. The effect of molecular structures of complexes on their FTIR spectral behavior was also discussed according to the actual X-ray structure.

References

Agwara, M.O., Ndifon, P.T., Ndosiri, N.B., Paboudam, A.G., Yufanyi, D.M., Mohamadou, A., 2010. Synthesis, characterization and antimicrobial activities of cobalt(II), copper(II) and zinc(II) mixed-ligand complexes containing 1,10-phenanthroline and 2,2'-bipyridine. Bull. Chem. Soc. Ethiop. 24 (3), 383–389.

Alan, H., John, Mc, Christine, J.M., 1997. Dichlorobis(1,10-phenanthroline-N, N')-cobalt(II)-Acetonitrile (1/1.5). Acta Cryst. C53, 723–725.

Ali, A.E., Saad, M.S., Mostafa, S.I., 2010. pH-Metric and spectroscopic properties of new 4-hydroxysalicylidene-2-aminopyrimidine Schiff-base transition metal complexes. J. Mol. Struct. 973, 69–75.

Bridges, S.M., Salin, M.L., 1981. Distribution of iron-containing superoxide dismutase in vascular plants. Plant Physiol. 68, 275–278.

Chyong, F.H., Hui, P., Cédric, B., Jadranka, T.-S., Paul, A., 2011. ABTS• + scavenging activity of polypyrrole, polyaniline and poly (3,4-ethylenedioxythiophene). Polym. Int. 60, 69–77.

Djuikom, S.Y.G., Divine, M.Y., Rajamony, J., Moise, O.A., 2016. Synthesis, characterization and antimicrobial properties of cobalt (II) and cobalt(III) complexes derived from 1,10-phenanthroline with nitrate and azide co-ligands. Inorg. Chem. 2, 1–16.

Dong, Z., Xiang-Ai, Y., Haibo, M., Xiaoxiong, L., Xizhang, W., Ziteng, L., Jing, M., 2018. Unexpected solvent effects on the UV/Vis absorption spectra of o-cresol in toluene and benzene: in contrast with non-aromatic solvents. R. Soc. Open. Sci., 5, 171928.

Elghamry, I., Youssef, M.M., Al-Omair, M.A., Elsawy, H., 2017. Synthesis, antimicrobial, DNA degradation and antioxidant activities of tricyclic sultams derivatives from saccharin. Eur. J. Med. Chem. 139, 107–113.

El-Sherif, A.A., Shehata, M.R., Shoukry, M.M., Barakat, M.H., 2012. Spectrochim. Acta A 96, 889.

Hassan, H.H., Amer, G., Mamdouh, S.M., 2006. Spectral regression and correlation coefficients of some benzaldimines and salicylaldimines in different solvents. Spectrochim. Acta Part A 63, 255–265.

Juan, R.A., Kysbel, M., Juan, C., 2018. Antibacterial activity of transition metal complexes with a tridentate NNO amoxicillin derived Schiff base. Appl. Organometal. Chem. 32 (7), e4374.

Kavanagh, F., 1963. Anal. Microbiology, Ch. 3 - Dilution Methods of Antibiotic Assays. Acad. Press, pp. 125–140.

Li, R.S., Lin, J.L., Zheng, Y.Q., 2004. Crystal structure of (carbonato-O, O')bis(l,10-phenanthroline-N, N')-cobalt(II) heptahydrate, [Co(C1$_2$H$_8$N2)2$_C$O3].$_7$H2O. Z. Kristallogr. NCS. 219, 425–426.

Mamdouh, S.M., Medhat, A.S., Alaa, E.A., Gehan, S.E., 2011. Solvatochromaticity and pH dependence of the electronic absorption spectra of some purines and pyrimidines and their metal complexes. Spectrochim. Acta Part A 79, 538–547.

Mashaly, M.M., El-Shafiy, H.F., El-Maraghy, S.B., Habib, H.A., 2005. Spectrochim. Acta A 61, 1853.

Masoud, M.S., Ali, A.E., Shaker, M.A., Elasala, G.S., 2012. Spectrochim. Acta A 90, 93.

Mensor, L.L., Menezes, F.S., Leitąo, G.G., Reis, A.S., dos Santos, T. C., Coube, C.S., Leitao, S.G., 2001. Screening of Brazilian plant extracts for antioxidant activity by the use of DPPH free radical method. Phytother. Res. 15, 127–130.

Mesut, G., Cihan, A., Belgin, E., 2013. Synthesis, characterization and antibacterial activity of 2-p-Tolyl-1H-Imidazo[4,5-f][1,10]phenanthroline and its Co(II), Ni(II) and Cu(II) complexes. Bull. Chem. Soc. Ethiop. 27 (2), 213–220.

Michael, J.Z., Hassan, H.H., Victor, Ch.K., 2007. The co-crystal of iron(II) complex hydrate with hydroxybenzoic acid: [Fe(Phen)$_3$]Cl (p-hydroxybenzoate).2(p-hydroxybenzoic acid).7H$_2$O. J. Chem. Crystall. 37 (3), 219–231.

Miller, F.A., Wilkins, C.H., 1952. Infrared spectra and characteristic frequencies of inorganic ions. Anal. Chem. 24 (8), 1253–1294.

Mohammad, M., Costantine, D., Essa, H., Sally, D., Samih, I., Eun, S. C., Babak, M., Hassan, H.H., 2015. Magnetic property, DFT calculation, and biological activity of bis[(l2-chloro)chloro(1,10-phenanthroline)copper(II)] complex. Chemico-Biol. Int. 23, 153–160.

Nikaido, H., 2009. Multidrug resistance in bacteria. Ann. Rev. Biochem. 78, 119–146.

Omer, A., Zuhal, Y., Orhan, B., 2010. (Carbonato-k^{2}O,O')bis(1,10-phenanthroline-k^{2}N,N')cobalt(III) nitratemonohydrate. Acta Cryst. E66, m46–m47.

Penumaka, N., Latha, J.N.L., Pallavi, P., Harish, S., Satyanarayana, S., 2006. Studies on antimicrobial activity of cobalt(III) ethylenediamine complexes. Can. J. Microbiol. 52 (12), 1247–1254.

Re, R., Pellegrini, N., Proteggente, A., Pannala, A., Yang, M., Rice-Evans, C., 1999. Antioxidant activity applying an improved ABTS radical cation decol¬orization assay. Free Radic Bio Med. 26 (9–10), 1231–1237.

Sambrook, J., Fritsch, E.F., Maniatis, T., 1989. Molecular Cloning: A Laboratory Manual. Cold Spring Harbor Laboratory Press, New York.

Tanwar, J., Das, S., Fatima, Z., Hameed, S., 2014. Multidrug resistance: an emerging crisis. Int. Perspect. Infect. Dis., 1–7 https://doi.org/10.1155/2014/541340. Article ID 541340.

Tomasz, A., 1994. New England J. Med. 330, 1247–1251.

Viganor, L., Howe, O., McCarron, P., McCann, M., Devereux, M., 2017. The antibacterial activity of metal complexes containing 1,10-phenanthroline: potential as alternative therapeutics in the era of antibiotic resistance. Curr. Top. Med. Chem. 17 (11), 1280–1302.

Youssef, M.M., Al-Omair, M.A., 2008. Cloning, purification, characterization and immobilization of L-asparaginase II from *E. coli* W3110. Asian J. Biochem. 3, 337–350.

Youssef, M.M., Arafa, R.K., Ismail, M.A., 2016. Synthesis, antimicrobial, and antiproliferative activities of substituted phenylfuranylnicotinamidines. Drug Des. Devel. Ther. 10, 1133–1146.

Zhu, H.L., Pan, Y.J., Wang, X.J., Yu, K.B., 2002. Crystal structure of tetraaqua(o-phenanthroline)cobalt(II) sulfate dihydrate, [C$_{12}$H$_8$N$_2$)Co(H$_2$O)$_4$]SO$_4$·2H$_2$O. Z. Kristallogr. NCS. 217, 601–602.